

Peak-peak correlations in the cosmic background radiation from cosmic strings

M. Sadegh Movahed^{1,2,3}, B. Javanmardi^{1,2}, Ravi K. Sheth^{3,4}

¹*Department of Physics, Shahid Beheshti University, G.C., Evin, Tehran 19839, Iran*

²*School of Astronomy, Institute for Research in Fundamental Sciences (IPM), P.O.Box 19395-5531, Tehran, Iran*

³*The Abdus Salam International Centre for Theoretical Physics, Strada Costiera, 11, Trieste 34151, Italy*

⁴*Center for Particle Cosmology, University of Pennsylvania, 209 S. 33rd St. Philadelphia, PA 19104, USA*

5 June 2019

ABSTRACT

We examine the two-point correlation function (TPCF) of local maxima in temperature fluctuations at the last scattering surface when this stochastic field is modified by the additional fluctuations produced by straight cosmic strings via the Kaiser–Stebbins effect. We demonstrate that one can detect the imprint of cosmic strings with tension $G\mu \gtrsim 1.2 \times 10^{-8}$ on noiseless $1'$ resolution CMB maps at 95% confidence interval. Including the effects of foregrounds and anticipated systematic errors increases the lower bound to $G\mu \gtrsim 9.0 \times 10^{-8}$ at 2σ confidence level. Smearing by beams of order $4'$ degrades the bound further to $G\mu \gtrsim 1.6 \times 10^{-7}$. Our results indicate that 2-point statistics are more powerful than 1-point statistics (e.g. number counts) for identifying the non-Gaussianity in the CMB due to straight cosmic strings.

Key words: Cosmic Microwave Background, two-point correlation function, cosmic strings, peaks, non-Gaussianity

1 INTRODUCTION

The origins of the seeds of present large scale structures in the universe are still debated. It is believed that they are mainly primordial and produced some time after Big-Bang. In this framework, there are two approaches: 1) the freezing-in of quantum fluctuations of a scalar field during the so-called inflationary epoch (Guth 1981; Liddle & Lyth 1993; Liddle 1999; Steinhard 1995); and/or 2) topological defects as sources (Kibble 1976; Kibble 1980). Indeed topological defects can be formed during phase transitions between different vacuum states in an expanding universe, and cosmic strings are predicted by quantum field theory in cosmology (Bevis et al. 2008, 2010; DePies 2009; Hindmarsh & Kibble 1995; Sakellariadou 2006; Vachaspati & Vilenkin 1984; Shellard 1987; Khlopov 1999; Vilenkin & Shellard 2000; Kibble 1976; Zeldovich 1980; Vilenkin 1981, 1985; Allen 1997). Both the inflationary and topological defects scenarios predict the same features for cosmic microwave background (CMB) power spectrum on large scales. But at the intermediate and small scales, due to differences in the super-horizon scale behavior of perturbations in these theories, the predictions are completely different.

The inflationary Λ CDM paradigm is consistent with today's high precision observations of the CMB. Nevertheless, from both theoretical and observational points of view there are many motivations for other sources of anisotropies.

E.g., in hybrid inflation models, the brane-world paradigm and superstring theory, production of topological defects are crucial and inevitable (Copeland et al. 1994; Sarangi & Tye 2002; Tye 2008; Kibble 2004; Copeland et al. 2004; Majumdar & Davis 2002; Pogosian et al. 2003; Dvali & Vilenkin 2004; Sakellariadou 1997). For more recent observational results see Bevis et al. (2008); Dvorkin et al. (2011); Ringeval & Bouchet (2012).

A cosmic string (CS) network which consists of infinite strings, loops and junctions of strings can generate gravitational waves as the universe evolves. Astrophysical evidence of CS depends on 1) the inter-commuting probability and 2) the dimensionless string tension $G\mu/c^2 \equiv \Lambda^2/M_{\text{Planck}}^2$, where G is Newton's constant, μ is the mass per unit length of the cosmic string and Λ is the energy scale of the string creation epoch (Bevis et al. 2008, 2010; Vilenkin & Shellard 2000). We set $c = 1$ throughout this paper. Determining bounds on the value of μ directly means limiting the basis of fundamental theories for CS production. In addition, observing cosmic strings not only is a kind of observational evidence for such theories, but also provides an opportunity to rule out or confirm theoretical models of particle physics.

There are many constraints on the upper as well as lower values of cosmic string parameters from theoretical and observational perspectives. Pulsar timing and photometry based on gravitational microlensing and gravitational waves require $10^{-15} < G\mu < 10^{-8}$ (Jenet et al.

2006; Pshirkov & Tuntsov 2010; Tuntsov & Pshirkov 2010; Damour & Vilenkin 2005; Battye & Moss 2010; Oknyanskij 1999; Gasilov et al. 1985; Blinnikov et al. 1982). The COSMOS survey requires $G\mu < 3 \times 10^{-7}$ (Christiansen et al. 2010). The 21cm signature of CS has been investigated in (Branderberger et al. 2010). The LIGO and VIRGO collaborations have determined $7 \times 10^{-9} < G\mu < 1.5 \times 10^{-7}$ (LIGO and VIRGO 2009). In a very recent paper, the stochastic gravitational waves from the European pulsar timing array place constrains $G\mu < 5.3 \times 10^{-7}$ (Sanidas et al. 2012).

Another strong constraint on $G\mu$ comes from the investigation of temperature fluctuations at the last scattering surface (Fraisse et al. 2008). The accumulation of anisotropies induced by CS on the fluctuations at last scattering surface can be divided into two categories: 1) anisotropies related to pre-recombination processes and created by the Kaiser-Stebbins effect (Kaiser & Stebbins 1984) and 2) the decay of string loops, which results in a stochastic background of gravitational waves (Fraisse et al. 2008; Kaiser & Stebbins 1984). CMB analyses bound the cosmic string tension to be $G\mu < 6.4 \times 10^{-7}$ (Battye & Moss 2010; Fraisse et al. 2008; Kaiser & Stebbins 1984; Fraisse 2005; Bevis et al. 2004; Bevis et al. 2007; Wyman et al. 2005, 2006; Perivolaropoulos 1993a). The effects of CS on the skewness of the one-point probability distribution of CMB temperatures (Yamauchi et al. 2010a), the TT power spectrum (Yamauchi et al. 2010b), the B-mode polarization (Ma & Brown 2010) have also been considered.

Various detection methods have been explored, including: Wavelet domain Bayesian denoising: $G\mu > 6.3 \times 10^{-10}$ (Hammond et al. 2008). The Canny algorithm: $G\mu > 5.5 \times 10^{-8}$ (Danos & Brandenberger 2010a; Stewart & Brandenberger 2009; Danos & Brandenberger 2010b). Level crossing analysis: $G\mu \gtrsim 4 \times 10^{-9}$ and $G\mu \gtrsim 5.8 \times 10^{-9}$ without and in the presence of instrumental noise, respectively (Movahed & Khosravi 2011).

More recent observational constraints via WMAP and the South Pole Telescope yield $G\mu < 1.7 \times 10^{-7}$ at 95% confidence interval (Dvorkin et al. 2011). Other computations expressed $G\mu < 0.7 \times 10^{-6}$ with $f_{\ell=10} < 0.11$ (the fractional contribution of cosmic string on the temperature power spectrum at $\ell = 10$) (Bevis et al. 2008). The constraints on CS from future CMB polarization come from (Foreman et al. 2011). The non-Gaussianity imposed by CS has been considered by (Starck, Aghanim and Forni 2004; Ringeval 2010; Hobson et al. 1999; Barreiro and Hobson 2001). By using the WMAP 7-year data release and the SPT $\ell < 3000$ power spectrum an upper limit on cosmic string tension has been given as $G\mu < 1.7 \times 10^{-7}$ at 95% confidence interval (Dvorkin et al. 2011). In the same paper, the aspect of polarization power spectrum to put robust constrains on the properties of CS have been discussed.

In the current study we concentrate on the discontinuities and fluctuations in the CMB map arising by CS from the Kaiser-Stebbins (KS) effect (Kaiser & Stebbins 1984). This phenomenon can produce observational consequences on the anisotropies in the CMB with high degree of reliability in the high resolution map. In what follows we study the two-point correlation function of local maxima or minima in the observed temperature maps (Bond & Efstathiou

1987; Heavens & Sheth 1999) to see if this is a useful probe of the extra roughness in the temperature distribution induced by strings. Previous work has shown that although the bispectrum of all pixels in a map at 5.5' resolution is not sensitive to a CS component, the two-point correlation function of local maxima is, especially on scales of order 10 – 20 arc-minutes (Heavens & Gupta 2001). The main goal of the present work is to quantify the limits of $G\mu$ which such a measurement can place.

Section 2 describes how we generate mock maps of primordial Gaussian CMB, and how we incorporate the effects of straight cosmic strings. In essence this is a straightforward combination of the algorithms in Heavens & Sheth (1999) with Movahed & Khosravi (2011). We then identify peaks in these maps and study if the one- and two-point statistics of these peaks agree with the Gaussian prediction, quantifying the statistical significance of the differences. A final section summarizes why we conclude that 2-point statistics are much more efficient for identifying the presence of CS compared to 1-point statistics.

2 SIMULATION AND ANALYSIS OF MOCK CMB MAPS

This section describes how we simulate maps of the last scattering surface (Stewart & Brandenberger 2009; Danos & Brandenberger 2010a,b; Perivolaropoulos 1993b; Moessner et al. 1994; Perivolaropoulos 1993a; Movahed & Khosravi 2011). At first, our code creates pure Gaussian fluctuations corresponding to the standard inflationary model with Λ CDM components in a flat universe following Bond & Efstathiou (1987). However, our program can be easily modified to other cosmological models for this purpose. Secondly, anisotropies produced by straight cosmic strings by the Kaiser-Stebbins effect, from the last scattering surface up to the present, are simulated following Perivolaropoulos (1993a) and Stewart & Brandenberger (2009); Danos & Brandenberger (2010a,b); Movahed & Khosravi (2011). Our method of simulation differs from that used to produce the CS maps analyzed by (Heavens & Gupta 2001), where the CS contribution to the energy-momentum tensor was modeled using Fourier methods (Pogosian et al. 1999).

For reasons discussed in detail in Stewart & Brandenberger (2009); Danos & Brandenberger (2010a,b); Movahed & Khosravi (2011), to simulate the Kaiser-Stebbins lensing due to moving cosmic strings we work in real space, where straight strings produce random jumps on the background radiation field. The scaling behavior of straight strings means that the number of strings crossing a given Hubble volume is fixed to $M_{\text{string}} = 10$ (Bennett & Bouchet 1988). The cosmic strings possess relativistic velocities; consequently, after $2t_H$ (t_H is the Hubble time) an entirely new network of cosmic strings provides new kicks to the CMB photons. The two signals are superposed, then smeared by our model of the instrumental beam, after which we add instrumental noise. Finally, we identify peaks in the simulated maps and measure the peak-peak correlation, showing results after averaging over a large ensemble of realizations.

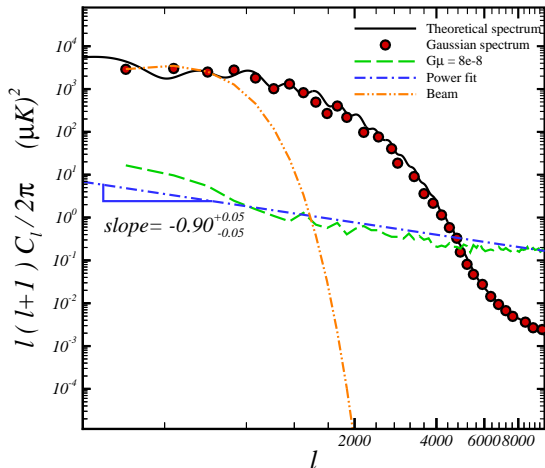


Figure 1. Contribution of various components to the total angular power spectrum of temperature fluctuations. Solid line shows the power-spectrum for a WMAP-7 Λ CDM model (from CAMB). Symbols show a simulated Gaussian map with resolution $R = 1'$ and size 10° . Long-dashed line shows the contribution from cosmic strings having $G\mu = 8 \times 10^{-8}$; dot-dashed line shows a power-law $\ell(\ell + 1)C_\ell \sim \ell^{-0.90 \pm 0.05}$. Dashed-dot-dot curve shows the window associated with a beam having FWHM = $20'$. Clearly, the CS component is most easily detected at $\ell \sim 6000$.

2.1 Mock Gaussian CMB map

In what follows, the size and resolution of simulated map are Θ and R , respectively. Thus, a $\Theta = 10^\circ$ map at $R = 1'$ requires 600×600 pixels. The rms instrumental noise, σ_{noise} , and the full width half maximum of detector, FWHM, are used to take into account additional effects on the simulated maps. We set $\sigma_{noise} = 10 \mu K$ which is appropriate for the South Pole Telescope (Ruhl et al. 2004; Keisler et al. 2011). We also use FWHM = $4'$ to illustrate our results.

For making Gaussian maps, all that is required is the initial power spectrum C_ℓ . For this, we use the CAMB software (Lewis et al. 2000) with parameters appropriate for a Λ CDM model that is consistent with the WMAP-7, Supernova type Ia (SNIa) and the Sloan Digital Sky Survey (SDSS) datasets. We use this C_ℓ to generate a 2D Gaussian random field following Bond & Efstathiou (1987). Since we are interested in relatively small angular scales, we work in the flat sky approximation, following Heavens & Sheth (1999).

To add the effects of strings we follow (Stewart & Brandenberger 2009; Danos & Brandenberger 2010a,b; Movahed & Khosravi 2011). This means that we ignore the contribution of CS loops, since their size is smaller than our map resolution (1 arcmin). In contrast the characteristic length scale of straight CSs is the Horizon scale.

2.2 Combination of simulated components

When combining the Gaussian (G) and string (S) components, we are careful to ensure that, at $\ell <$

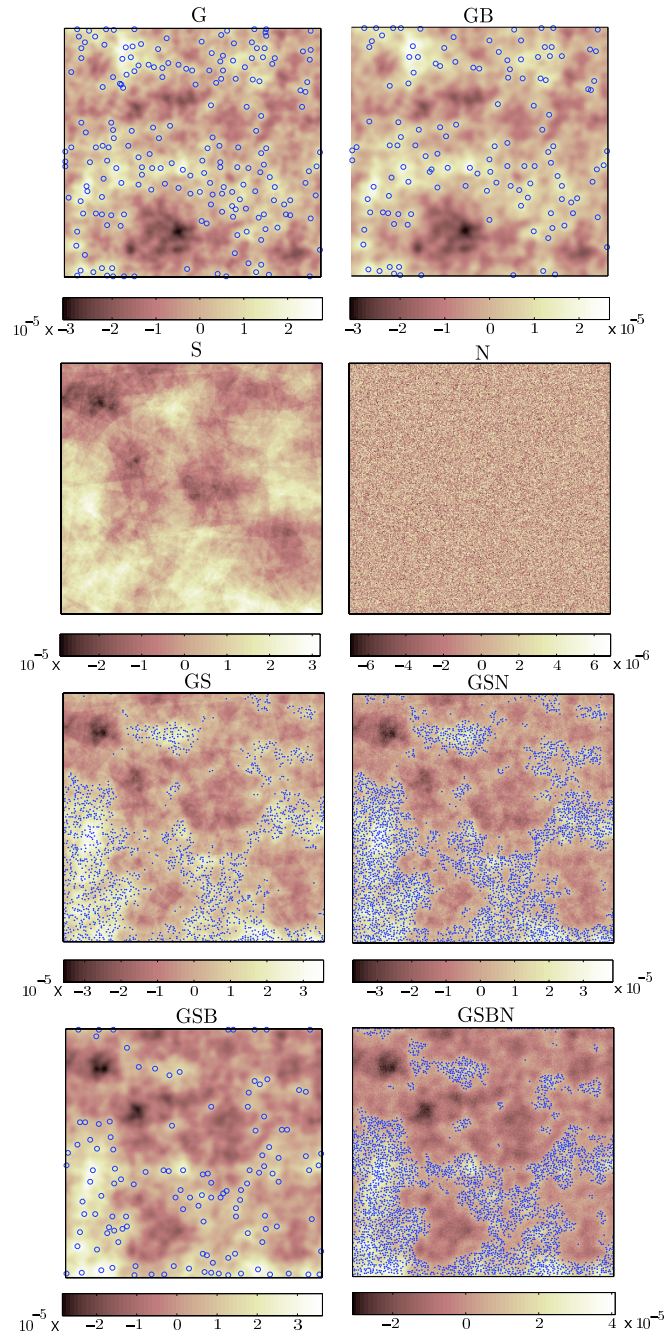


Figure 2. Various components of simulated maps, for a WMAP-7 Λ CDM model, with $G\mu = 8 \times 10^{-7}$ strings. The map size is $5^\circ \times 5^\circ$ at resolution $R = 1'$ and smeared by a beam of FWHM = $4'$. Circles in some panels show peaks above $\vartheta = 0.5\sigma_0$.

200 (Danos & Brandenberger 2010a; Movahed & Khosravi 2011), the total power is the same as that observed. In practice, this means that in each pixel (i, j) we set the fluctuation, $\mathcal{F} \equiv (T(i, j) - \langle T \rangle) / \langle T \rangle$, to be

$$\mathcal{F}_{(G+S)}(i, j) = \omega \mathcal{F}_{(G)}(i, j) + \mathcal{F}_{(S)}(i, j) \quad (1)$$

where $\omega < 1$ is chosen so that the amplitude of the power spectrum

$$C_\ell^{(G+S)} = \omega^2 C_\ell^{(G)} + C_\ell^{(S)} \quad (2)$$

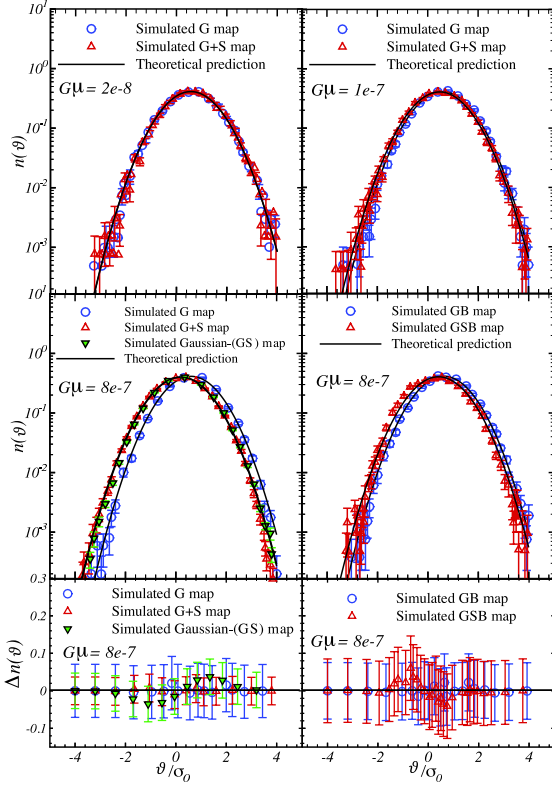


Figure 3. Abundance of density of peaks as a function of peak threshold level for pure Gaussian maps and upon adding a cosmic string component. Upper left: $G\mu = 2 \times 10^{-8}$. Upper right: $G\mu = 1 \times 10^{-7}$. Middle left: $G\mu = 8 \times 10^{-7}$. Results for a Gaussian map (Gaussian-(GS)) having the same power spectrum as the Gaussian+String map has also been indicated in this panel. Middle right: for $G\mu = 8 \times 10^{-7}$ with beam effect. The lower panels show the difference between theoretical Gaussian field prediction for the number density of peak and what measured in the simulated maps.

is close to that observed at $\ell < 200$. Since $C_\ell^{(S)}$ depends on ℓ , determination of the appropriate value of ω is done by a likelihood analysis.

The beam smearing is modeled by:

$$C_\ell^{(G+S)B} = C_\ell^{(G+S)} e^{-\Gamma^2 \ell(\ell+1)} \quad (3)$$

with $\Gamma = \text{FWHM}/\sqrt{8 \ln 2}$ (Bond & Efstathiou 1987; Heavens & Sheth 1999).

Finally, we add a model for the noise:

$$\mathcal{F}(i, j) \equiv \mathcal{F}_{(G+S)B}(i, j) + \mathcal{F}_{(N)}(i, j), \quad (4)$$

where the final noise term is white, i.e., it has $\langle \mathcal{F}_{(N)}(\mathbf{r}_1) \mathcal{F}_{(N)}(\mathbf{r}_2) \rangle \sim \delta_{\text{Dirac}}(\mathbf{r}_1 - \mathbf{r}_2)$, with the noise in pixel (i, j) being a zero-mean Gaussian number with rms σ_{noise} . Figure 2 illustrates various components and steps in our map making process.

2.3 Peak counts in mock maps

We have checked that the number density of peaks we identify in the Gaussian maps agrees with that expected from theory. When the peak height is expressed in units of the

rms temperature, $\vartheta = \Delta T/T$, this prediction depends only on the shape of the power spectrum C_ℓ (Bond & Efstathiou 1987). Since CS modify C_ℓ at high ℓ , it is interesting to ask if the peak counts predicted by $C_\ell^{(G+S)}$ provide a good description of the peak abundances in the $G+S$ maps, even though the maps themselves are not Gaussian. If not, then peak counts alone allow one to distinguish between a purely Gaussian model and one with an additional component.

Figure 3 shows that, for $G\mu \leq 10^{-7}$ (top panels), the peak counts in G and $G+S$ are almost indistinguishable. For larger values of $G\mu$, the peak counts are noticeably different from one another (middle left panel), with the distribution being shifted to smaller mean values when CS are present. However, the measurements are each well described by Gaussian peaks theory (Bond & Efstathiou 1987) with their respective power spectra ($C_\ell^{(G)}$ for the circles, and $C_\ell^{(G+S)}$ for the triangles), even though the $G+S$ maps themselves are not Gaussian. Thus, given only the observed C_ℓ and the peak counts, it will not be possible to determine if there is a CS component in the maps. Beam smearing makes the counts indistinguishable upto even larger values $G\mu \leq 8 \times 10^{-7}$ (middle right panel of Figure 3). In addition, to make more obvious, we have added $\Delta n(\vartheta) \equiv n_{\text{com.}}(\vartheta) - n_{\text{the.}}(\vartheta)$ in the lower panel of Figure 3. Where "com." refers to numerical result and "the." corresponds to theoretical prediction.

Recently, Pogosyan et al. (2011) derived expressions for the number density of extrema in weakly non-Gaussian 2-Dimensional fields. They showed that various non-Gaussian models could be distinguished by means of $n(\vartheta)$. Our analysis demonstrates that, at least for the non-Gaussianity due to straight CSs, this does not work.

2.4 Two-point statistics

Although we have demonstrated that peak counts in our $G+S$ maps are consistent with those in a Gaussian field having the same C_ℓ , direct inspection of the maps themselves (top panel of Figure 4) shows that they have quite different morphologies. The CS component seems to add small scale random noise on top of the original Gaussian CMB signal. We turn therefore to the use of two-point peak statistics for distinguishing between the two maps.

To this end, we measure the TPCF of peaks in our Gaussian maps, our $G+S$ maps, and our Gaussian-GS maps. For each value of $G\mu$, map size, resolution scale and beam size, we have generated ensembles of ~ 100 maps. Lower panel of Figure 4 and Figure 5 show results from averaging over 100 realizations of maps with $\Theta = 10^\circ$ map at $R = 1'$ and $\vartheta > 1\sigma_0$. There are obvious differences between the TPCF in the G and $G+S$ maps, with the latter having substantially more signal on small scales. Although the beam erases some of this (Figures 4 and 5), a residual effect remains. This signal is rather different from that measured in a Gaussian field which has the same C_ℓ (what we called Gaussian-GS previously). So we conclude that this is indeed a promising method for identifying the CS component in the maps.

The lower panel of Figure 4 shows explicitly that, although the peak counts were unable to distinguish between GSB and Gaussian-GSB maps (Figure 3), the TPCF on

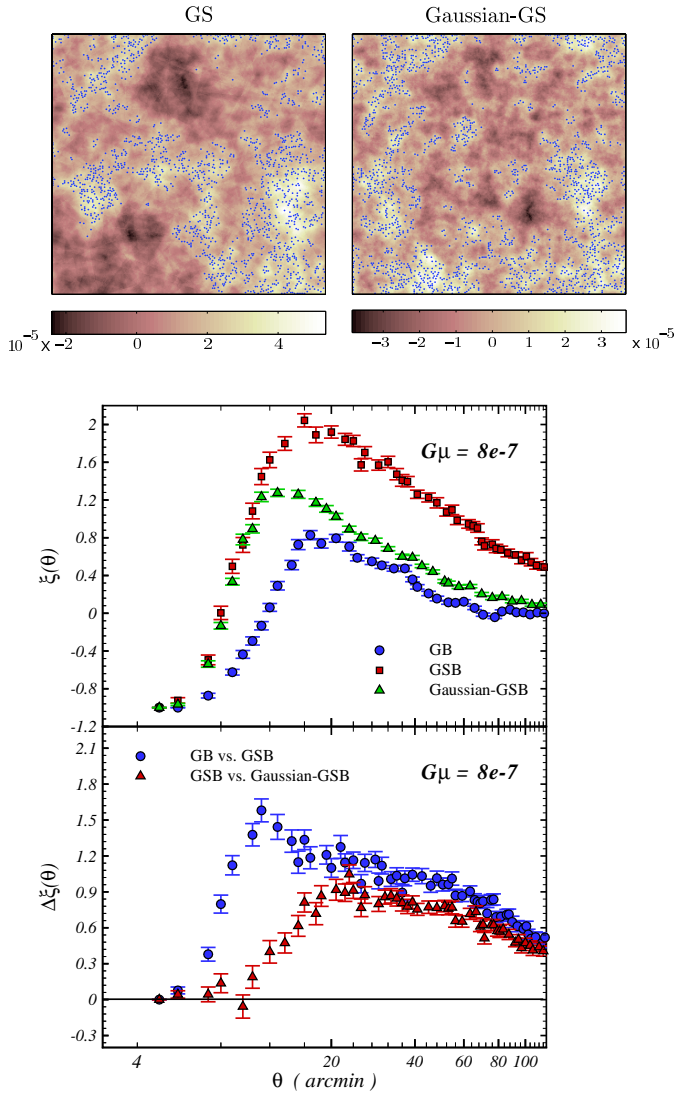


Figure 4. Upper panel: Comparison of a Gaussian+String map (left) with a pure Gaussian map which has the same total power spectrum (right); blue dots show peaks above $\vartheta = 0.5\sigma_0$. In both cases, $G\mu = 8 \times 10^{-7}$, the resolution $R = 1'$ and the map size shown is $5^\circ \times 5^\circ$. The morphology of these two maps is quite different. Lower panels: TPCF of $\vartheta = 1.0\sigma_0$ peaks in these maps and differences between them.

scales $\theta \geq 12'$ can. Figure 5 shows that the ability to discriminate depends on $G\mu$ and the beam size FWHM.

2.5 Quantitative limits

To quantify this we first compute the Student's t-test based on:

$$t(\theta) = \frac{\xi_{(\diamond)}(\theta) - \xi_{(\otimes)}(\theta)}{\sqrt{\sigma_{(\diamond)}^2(\theta) + \sigma_{(\otimes)}^2(\theta)}} \quad (5)$$

where $\xi(\theta)$ is the TPCF and $\sigma(\theta)$ is the mean standard deviation of each term in the numerator. The symbols \diamond and \otimes correspond to the $G + S$ and G measurements and to $(G + S)B$ and $(G)B$ with beam effect. For each θ , the corre-

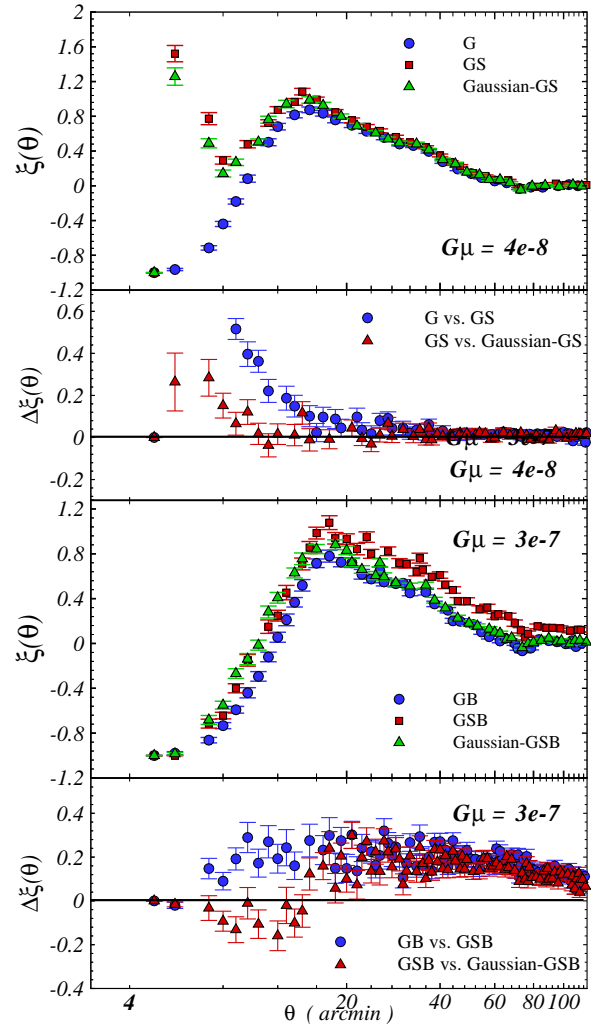


Figure 5. Two-point correlation function of peaks above $\vartheta = 1\sigma_0$ for different values of $G\mu$. Here FWHM is $4'$. $\Delta\xi(\theta)$ corresponds to difference between TPCF of various cases indicated in plots.

sponding P-value, $p(\theta)$, are calculated. Degrees of freedom based on the t -distribution function are $2N_{sim} - 2$, where N_{sim} is the number of simulated maps.

We then define $\chi^2 \equiv -2 \sum \ln p(\theta)$. The final P-value related to χ^2 is calculated based on chi-square distribution function with $2(\theta_{max} - \theta_{min})/\Delta\theta - 2$ degrees of freedom. Fig. 6 shows this P-value as a function of $G\mu$ for various maps with $\Theta = 10^\circ$. We have drawn lines at $p = 0.0027$, and 0.0455 , since these correspond to 3σ and 2σ significance levels. This shows that the TPCF can detect CS at 95%CL provided $G\mu \gtrsim 1.2 \times 10^{-8}$ in maps without instrumental noise. If noise is present, with rms $\sigma_{noise} = 10\mu\text{K}$, then this limit increases to $G\mu \gtrsim 9.0 \times 10^{-8}$. Including beam smearing further degrades our limits: the minimum detectable CS becomes $G\mu \gtrsim 1.6 \times 10^{-7}$ at 2σ confidence interval. Table 1 summarizes our results.

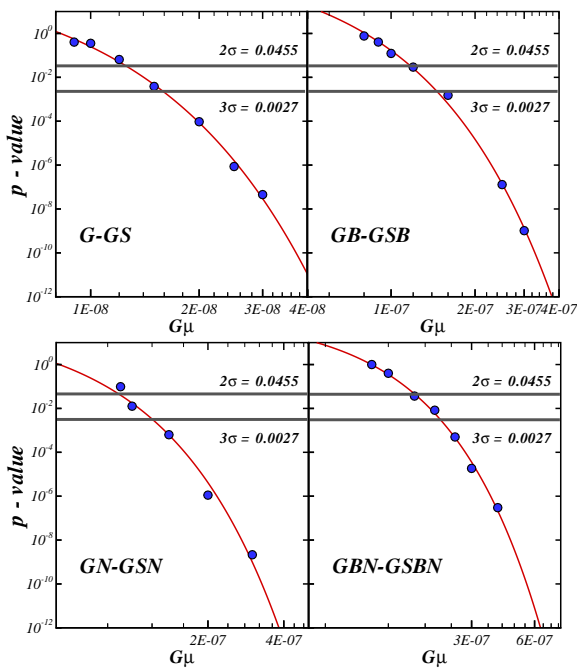


Figure 6. P-value as a function of $G\mu$. Upper left panel indicates the result for Gaussian CMB map. The effect of beam on the capability of TPCF to detect CS has been shown in upper right panel. Lower left panel corresponds to P-value for map in the presence of instrumental noise. The effect of finite beam size and instrumental noise have been indicated in lower right panel. To determine each point in this plot we did average on at least 100 ensembles.

3 CONCLUSION

If they exist, cosmic strings are expected to leave an imprint in the CMB. We argued that although such strings may alter the power spectrum (Figure 1) and the statistics of hot and cold spots (Figure 2), the change to the one-point statistics of peaks in CMB maps cannot be distinguished from that for a Gaussian field having the same power spectrum (Figure 3). On the other hand, the two-point statistics show differences (Figures 4 and 5) which we believe can be used to reject the hypothesis that the map is a purely Gaussian (Figure 6).

We argued that CS will be detected at high significance only if the string tension is sufficiently high: $G\mu \gtrsim 1.2 \times 10^{-8}$. Accounting for the fact that instrumental noise complicates the measurement increases this limit to $G\mu \gtrsim 9.0 \times 10^{-8}$ (Figure 6 and Table 1). The CS signal is particularly strong on arcminute and smaller scales. Some of this signal is removed if the beam size of the experiment is larger than this scale. For a $4'$ beam, the limit is $G\mu \gtrsim 1.2 \times 10^{-7}$ at 2σ confidence interval. Broader beams increase the limiting $G\mu$ further.

We have argued that two-point statistics of peaks (the pair correlation function) are better than one-point statistics (peak number counts) for distinguishing between models. Our results suggest that the n -point correlation functions of peaks can be used for similar purpose. This is interesting in view of previous work showing that the 3-point statistics of all pixels is not very informative.

Map	2σ	3σ
G-GS	$G\mu \gtrsim 1.2 \times 10^{-8}$	$G\mu \gtrsim 1.6 \times 10^{-8}$
GN-GSN	$G\mu \gtrsim 9.0 \times 10^{-8}$	$G\mu \gtrsim 1.2 \times 10^{-7}$
GB-GSB	$G\mu \gtrsim 1.2 \times 10^{-7}$	$G\mu \gtrsim 1.5 \times 10^{-7}$
GBN-GSBN	$G\mu \gtrsim 1.6 \times 10^{-7}$	$G\mu \gtrsim 2.2 \times 10^{-7}$

Table 1. Limits on $G\mu$ which come from analysis of the differences between the TPCF for maps with and without cosmic strings, when $R = 1'$, FWHM= $4'$ and $\sigma_{noise} = 10\mu K$.

Final remark is that it could be interesting to use more realistic models (Landriau & Shellard 2003; Fraisse et al. 2008; Landriau & Shellard 2010) to simulate a map taking all contributions of cosmic strings into account and apply our method to examine the effect of cosmic strings in our future works. Also, it is useful to apply this method to discriminate the effect of generic cosmic strings and superstrings.

ACKNOWLEDGMENTS

MSM is grateful to the Office of Associates at ICTP and the hospitality of HECAP section of ICTP. MSM and BJ are grateful to H. Moshafi for preparing some power spectra. BJ thanks Mr. Mehran Yazdizadeh for his help with computing. We acknowledge the use of CAMB software, WMAP-7, the SNLS gold sample and the Two Degree Field Galaxy Redshift Survey (2dFGRS) data sets. MSM thanks the Shahid Beheshti University research deputy affairs which supported this work by grant No. 600/1037.

REFERENCES

- Allen B., "Relativistic gravitation and gravitational radiation", J.-A. Marck, J.-P. Lasota. (Proceedings, Les Houches School of Physics: Astrophysical Sources of Gravitational Radiation), Cambridge Contemporary Astrophysics, 1997, pages 373-417, gr-qc/9604033 (1996).
- Bardeen J.M., J.R. Bond, N. Kaiser and A.S. Szalay, *Astrophys. J.* **304**:15-61 (1986).
- Battye R. and Moss A., arXiv:1005.0479.
- Bennett D.P. and Bouchet F.R., *Phys. Rev. Lett.* **60** (1988) 4.
- Bevis N., Hindmarsh M., Kunz M. and Urrestilla J., *Phys. Rev. Lett.* **100**, (2008) 021301, astro-ph/0702223.
- Bevis N., Hindmarsh M., Kunz M. and Urrestilla J., *Phys. Rev. D.* **82**, (2010) 065004, arXiv:1005.2663.
- Bevis N., Hindmarsh M. and Kunz M., *Phys. Rev. D* **70**, (2004) 043508.
- Bevis N., Hindmarsh M., Kunz M. and Urrestilla J., *Phys. Rev. D* **75**, 065015 (2007).
- Blinnikov S. I. and Khlopov M. Yu., *Yadernaya Fizika* (1982) V. 36, PP. 809-811. [English translation: *Sov.J.Nucl.Phys.* (1982) V. 36, PP. 472-474].
- Bond J. R. and Efstathiou G., *Mon. Not. Roy. Astron. Soc.* **226**, 655-687, 1987.
- Christiansen J.L. et al. arXiv: 1008.0426.

- Branderberger R.H., Danos R.J., Hernandez O.F. and Holder G.P., JCAP **12** (2010) 028.
- Copeland E., Liddle A. R., Lyth D. H., Stewart E. D., Wands D., Phys. Rev. D **49** (1994) 6410-6433.
- Copeland E. J., Myers R. C., Polchinski J., JHEP **0406:013,2004**, arXiv:hep-th/0312067.
- Damour T. and Vilenkin A., Phys. Rev. D **71**, 063510 (2005), arXiv:hep-th/0410222.
- Danos R.J. and Brandenberger R.H., Int. J. Mod. Phys. **D 19** (2010) 183.
- Danos R. J. and Brandenberger R. H., JCAP, **02**, pp. 033 (2010), arXiv:0910.5722.
- Davis M. and Peebles P. J. E., ApJ, **267**, 465, 1983.
- DePies M., Dissertations P. and Theses 2009. Section 0250, Part 0606 140 pages; [Ph.D. dissertation].United States – Washington: University of Washington; 2009. Publication Number: AAT 3370485. Source: DAI-B 70/08, Feb 2010, arXiv:0908.3680.
- Dvali G. and Vilenkin A., JCAP **0403**, 010 (2004).
- Dvorkin C., Wyman M. and Hu W., Phys.Rev.D.**84**:123519 (2011).
- Fatemi-Ghomi N., Palmer P.L. and Petrou M., J. Math. Imaging Vis. **10** 7-25 (1999).
- Foreman S. , Moss A. and Scott D., Phys.Rev.D **84**:043522 (2011).
- Fraisse A. A., Ringeval C., Spergel D. N. and Bouchet F. R., Phys. Rev. D **78**, 043535 (2008).
- Fraisse A. A., arXiv:astro-ph/0503402.
- Fraisse A.A. , Ringeval C., Spergel D.N. and Bouchet F.R., Phys. Rev. **D 78** (2008) 043535.
- Gasilov V. A., Maslyankin V. I. and Khlopov M. Y., Astrofizika (1985), V.23, PP.191-201. [English translation: Astrophysics, V.23, NO.1/JAN, PP. 485-491, 1986].
- Guth A. H., Phys. Rev. D **23**, 347 (1981).
- Hamilton A. J. S., ApJ, **417**, 19, 1993.
- Hammond D.K., Wiaux Y. and Vandergheynst P., arXiv:0811.1267.
- Heavens A.F. and Sheth R.K., Mon. Not. Roy. Astron. Soc. **310** (1999) 1062.
- Heavens A. F. and Gupta S., Mon.Not.Roy.Astron.Soc. **324** (2001) 960.
- S.-H. Henry Tye, Lect. Notes Phys. **737**:949-974, 2008, arXiv:hep-th/0610221.
- Hewett P. C., M, **201**, 867(1982).
- Hindmarsh M. and Kibble T. W. B., Rept. Prog. Phys. **58**:477-562,1995, hep-ph/9411342.
- Jenet F. A., Hobbs G. B., Straten W. V., Manchester R. N., Bailes M., Verbiest J. P. W., Edwards R. T., Hotan A. W., Sarkissian J. M. and Ord S. M., Astrophys. J. **653**, 1571 (2006), astro-ph/0609013 (2006).
- Hobson M.P., Jones A.W. and Lasenby A.N., Mon.Not.Roy.Astron.Soc, **309**, Issue 1, 125(1999).
- Barreiro R.B. and Hobson M.P., Mon.Not.Roy.Astron.Soc. **327**, 813(2001).
- Kaiser N. and Stebbins A., Nature **310** (1984) 391.
- Keisler R. et al., arXiv:1105.3182.
- Kerscher M., Szapudi I. and Szalay A. S., The Astrophysical Journal, **535**, Issue 1, L13-L16 (2000).
- Khlopov M. Y., "COSMO PARTICLE PHYSICS", World Scientific publication (1999).
- Kibble T. W. B., Topology Of Cosmic Domains And Strings, J. Phys. A **9**, 1387 (1976).
- Kibble T. W. B., Physics Reports, **67**, 183 (1980).
- Kibble T. W. B., arXiv:astro-ph/0410073.
- M. Landriau M. and Shellard E. P. S., Phys. Rev. D **67**, 103512 (2003).
- M. Landriau M. and Shellard E. P. S., Phys.Rev. D **83**, 043516 (2011).
- Landy S. D. and Szalay A. S., ApJ, **412**, L64, 1993.
- Larson D. L., Wandelt B. D., arXiv:astro-ph/0505046.
- Larson D. et al., Astrophys. J. Suppl. **192** (2011) 16.
- Lewis A., Challinor A. and Lasenby A., Astrophys. J. **538**(2000) 473.
- Liddle A. R. and Lyth D. H., Phys. Rep **231**, 1 (1993).
- Liddle A. R., To appear, proceedings of ICTP summer school in high-energy physics, 1998, arXiv:astro-ph/9901124.
- LIGO and VIRGO collaboration, Nature **460** (2009)20.
- Lumsden S. L., Heavens A.F., Peacock J.A., Mon. Not. R. ast. Soc. **238**, 293-318, 1989.
- Ma Y.Z., Zhao W. and Brown M.L., JCAP **10** (2010)007.
- Majumdar M. and Davis A.C., JHEP, **0203**, 056 (2002).
- R. Moessner R., Perivolaropoulos L. and Brandenberger R., Ast. Phys. J. **425**, 365 - 371 (1994).
- Movahed M. S. and Khosravi S., JCAP **1103**:012 (2011) arXiv:1011.2640.
- Oknyanskij V. L., Gravit. Cosmol., Vol. 5, suppl. issue, p. 97 - 102 (1999).
- Peacock J.A. and Heavens A.F., Mon. Not. Roy. Astron. Soc. **217** (1985) 805-820
- Peebles P.J.E., *The Large-Scale Structure of the Universe*, Princeton University Press, 1980.
- Pen U.-L., Seljak U., Turok N., Phys. Rev. Lett., **79**, 1611 (1997).
- Perivolaropoulos L., Phys. Lett. **B 298** (1993) 305.
- Perivolaropoulos L. , Phys. Rev. D **48**, 4 (1993).
- Pogosian L. and Vachaspati T., Phys. Rev. D **60**, 083504 (1999).
- Pogosian L., Tye S., Wasserman I. and Wyman M., Phys. Rev. D **68**, 023506 (2003).
- D. Pogossyan, C. Pichon and C. Gay, Phys. Rev. D, **84**, 083510 (2011).
- Pshirkov M. S. and Tuntsov A. V., Phys. Rev. D, **81**, 083519 (2010), arXiv:0911.4955.
- Ringeval C., Advances in Astronomy, vol. 2010, Article ID 380507, 28 pages, 2010.
- Ringeval C. and Bouchet F. R., arXiv:1204.5041.
- Rice, S. O., *Selected papers on Noise and Stochastic Processes*, p. 133, ed. Wax, N., Dover, 1954.
- Ruhl J. E. et al. (The SPT) (2004), arXiv:astro-ph/0411122.
- Sakellariadou M., International Journal of Theoretical Physics, Vol. 36, No. 11 (1997).
- Sakellariadou M., Lect. Notes Phys.**718**:247-288,2007, hep-th/0602276 (2006).
- Sanidas Sotirios A., Battye Richard A. and Stappers Benjamin W., arXiv:1201.2419 .
- Sarangi S., S.-H. Henry Tye, Phys.Lett. B **536** (2002) 185-192.
- Seljak U. and Zaldarriaga M., Ap. J. **469**, 437 (1996).
- Seljak U., Ap. J. **482**, 6 (1997).
- Shellard E. P. S., Nucl. Phys. B **283**, 624 (1987).
- Starck J. L., Aghanim N. and Forni O., Astron.Astrophys. **416** (2004) 9-17, arXiv:astro-ph/0311577.

- P. J. Steinhard, Cosmology at the crossroads, in Particle and Nuclear Astrophysics and Cosmology in the Next Millennium, E. W. Kolb and R. Peccei, eds., World Scientific, Singapore.
- Stewart A. and Brandenberger R.H., JCAP **02** (2009) 009.
- Szapudi I. and Szalay A. S., Astrophysical Journal Letters, 494, L41 (1998).
- Tojeiro R., Castro P. G., Heavens A. F. and Gupta S., Mon. Not. Roy. Astron. Soc. 365, 265-275 (2006).
- Tuntsov A. V. and Pshirkov M. S., Phys. Rev. D, 81, 063523 (2010), arXiv:1001.4580.
- Vachaspati T. and Vilenkin A., Phys. Rev. D 30 2036 (1984).
- Vilenkin A., Phys. Rep., 121 263 (1985).
- Vilenkin A. and Shellard E. P. S., Cosmic Strings and Other Topological Defects (Cambridge, UK: Cambridge University Press. ISBN 0521654769. pp. 578, 2000).
- Vilenkin A., Cosmological Density Fluctuations Produced By Vacuum Strings, Phys. Rev. Lett. 46, 1169 (1981). [Erratum-ibid. 46, 1496 (1981)].
- Wyman M., Pogosian L. and Wasserman I., Phys. Rev. D 72, 023513 (2005).
- Wyman M., Pogosian L. and Wasserman I., Phys. Rev. D 73, 089905(E) (2006).
- Yamauchi D. et al. JCAP **05** (2010) 033.
- Yamauchi D., Takahashi K., Sendouda Y., Yoo C. M. and Sasaki M., arXiv:10060687.
- Zeldovich Y. B., Cosmological fluctuations produced near a singularity, Mon. Not. Roy. Astron. Soc. 192, 663 (1980).